

# The effect of groundwater fluctuations on the velocity pattern of slow-moving landslides

Th. W. J. van Asch<sup>1,3</sup>, J.-P. Malet<sup>2</sup>, and T. A. Bogaard<sup>3</sup>

<sup>1</sup>Utrecht University, Faculty of Geosciences, Utrecht, The Netherlands

<sup>2</sup>School and Observatory of Earth Sciences, Institute of Earth Physics, CNRS & University of Strasbourg, Strasbourg, France

<sup>3</sup>Delft Univ. of Technology, Water Resources Section, Faculty of Civil Engineering and Geosciences, Delft, The Netherlands

Received: 8 September 2008 – Revised: 13 May 2009 – Accepted: 13 May 2009 – Published: 18 May 2009

**Abstract.** Slow-moving landslides show complex mechanical and fluid interactions. They show among others non linear intrinsic viscosity of the shear zone, undrained loading effects and the generation of excess pore water pressure. The parameterization of hydrological and geomechanical factors by field and laboratory tests to describe the movement pattern of these landslides is difficult. It is a challenge to simulate accurately the de- and acceleration of these landslides and particularly, to forecast catastrophic surges.

In this paper the relation between groundwater fluctuation and landslide velocity for two deep-seated landslides of the Trièves Plateau (the Monestier-du-Percy landslide and the Saint-Guillaume landslide) is analysed. Inclinator measurements, showing the displacement in depth after 1–2 months periods, showed on both landslides shear band deformation within 1 m. At the Monestier-du-Percy landslide, depending on the position, the shear band depths vary between 25.0 m and 10.0 m. At the Saint-Guillaume landslide, the inclinometers detected several slip surfaces inside the clays, at respectively 37.0 m, 34.5 m, and 14.0 m depth. Two simple geomechanical models are developed to describe these displacements in depth in relation to measured groundwater fluctuations. Calibration of the models using the friction angle delivered no constant values for different measuring periods. It appeared that calibrated (apparent) friction values increase with increasing groundwater levels. The paper discusses the possibility of the generation of negative excess pore water pressures as a feed back mechanism, which may explain the complex displacement pattern of these landslides developed in varved clays.

## 1 Introduction

In the French Alps, hundreds of landslides have occurred in the varved clays of the Trièves Plateau, around 50 km south of Grenoble (Fig. 1a). These clays are glacio-lacustrine sediments deposited in glacially dammed lakes during the Würm maximum episode, and are characterised by an alternation of silt laminae of 1–20 mm in thickness (Giraud et al., 1991; van Asch et al., 1996). The activity of most of these landslides is seasonal (van Genuchten, 1989; van Asch et al., 1996): the movements are triggered by snowmelt and rainfall especially in spring time. Human activity may also have favoured the instability of some landslides like the Mas Avignonet and Harmalières landslides, which are located in the Drac valley (Fig. 1) and have been triggered by the filling of the Monteynard dam (Lorier and Desvarreux, 2004). The landslides developed in varved clays show a complex style of deformation with both internal strains in the landslide body and sliding processes along slip surfaces which may be shallow (4 to 8 m) or more deep-seated (20 to 40 m) (Antoine et al., 1981). Slope stability calculations indicate that the groundwater levels of the deep-seated slides have to rise nearby the topographic surface in order to trigger or accelerate the movements (Vuillermet, 1992).

The aim of this paper is to analyse quantitatively the relation between groundwater fluctuations and landslide velocity for two deep-seated landslides of the Trièves Plateau: the Monestier-du-Percy landslide (Giraud et al., 1980), and the Saint-Guillaume landslide (Azimi et al., 1994; Méric et al., 2007). First, the environmental settings of the landslides are described. Second, two kinematical displacement models (a Janbu model – M1, and an equation of motion model – M2) are presented. Third, the field observations (displacement and groundwater level) are analysed, and modelled. Finally, the paper discusses their complex displacement pattern and



Correspondence to: J.-P. Malet  
(jeanphilippe.malet@eost.u-strasbg.fr)

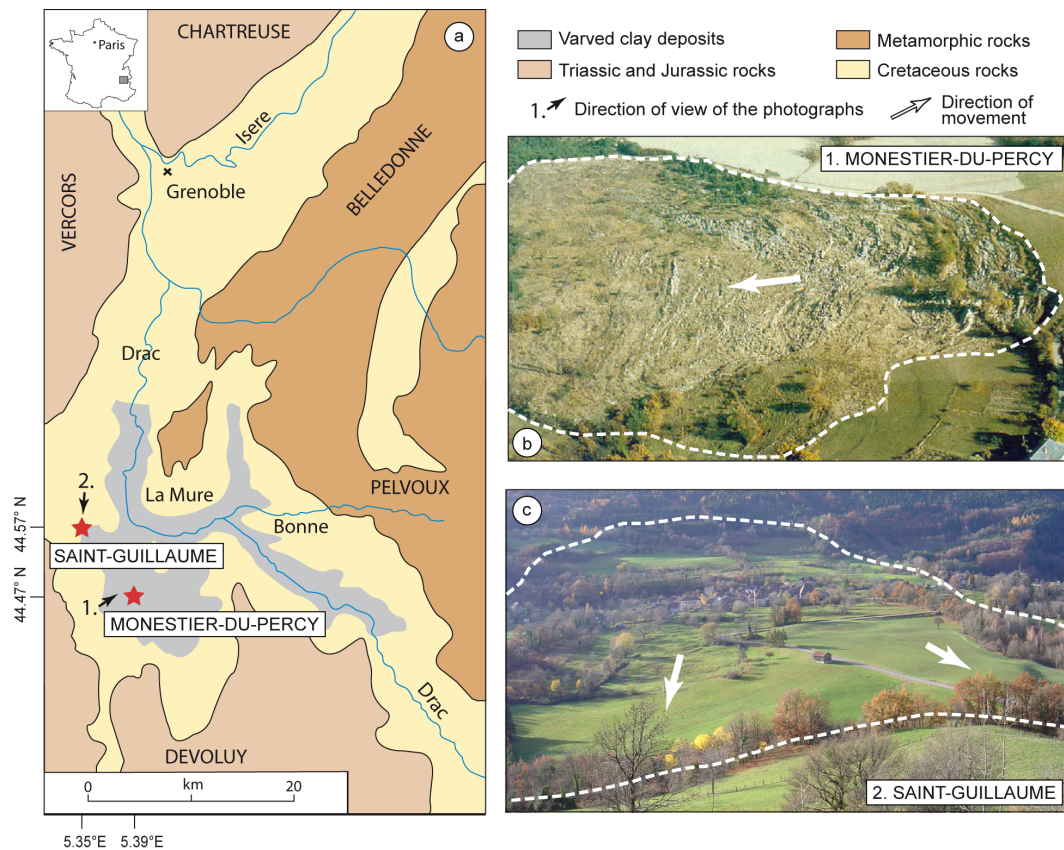


**Fig. 1.** (a) Simplified geological map of the Trièves Plateau and the surroundings, showing the maximum extension of glacier (Würm II period), the extent of the varved clay deposits, and the location and photographs of the (b) Monestier-du-Percy landslide (in 1981) and the (c) Saint-Guillaume landslide (in 2005).

stresses the importance of negative excess pore water pressures on their kinematics.

## 2 Geomorphological, geologic and geotechnical settings of the landslides

### 2.1 The Monestier-du-Percy landslide

The Monestier-du-Percy landslide (also called “Serre des Bayles” landslide) was reactivated on 9 April 1978. The geomorphological analysis of aerial photographs (1948, 1956, 1993, 2003) indicated instability signs of the landscape since 1948 with the presence of small scarps and lobes along the slopes. The landslide affects an area of approximately 0.9 km<sup>2</sup>, with a relatively low-gradient slope (12°), and the land cover is mainly composed of pasture lands (Fig. 1b). The geology of the site is composed of approximately 40 m of varved clays which overlay a bedrock of Oxfordian clay-shales with a dip of approximately 40° in the South-West direction, whilst the landslide is developing in the North-West direction (Antoine et al., 1981).

The meteorological triggering conditions associate heavy rains in the two months preceding the onset of the failure (203 mm in February 1978 and 197 mm in March 1978, whilst the average rainfall is 155 mm per month for this period of the year), and a rapid melt of snow cover.

Geomorphological observations and analysis of the geotechnical drillings indicate a rotational movement in the upper part of the landslide, and a translational movement in the lower part imposed by a flattening of the slip surface in the down slope direction. Open pits and geotechnical drillings indicate the presence of alluvial deposits with a thickness of 1.5 to 2.0 m above the main scarp (Fig. 2). These alluvial deposits are draining a swamp area located on the South-East of the landslide (Fig. 2). One piezometer (P1), three inclinometers (I1, I2, I3), and 12 topographical benchmarks have been installed in order to better understand the mechanics and monitor the displacements and the hillslope hydrology (Fig. 2).

The landslide mass can be divided in two parts bordered by a positive undulation of the clay-shale bedrock in the South-West–North-East direction:

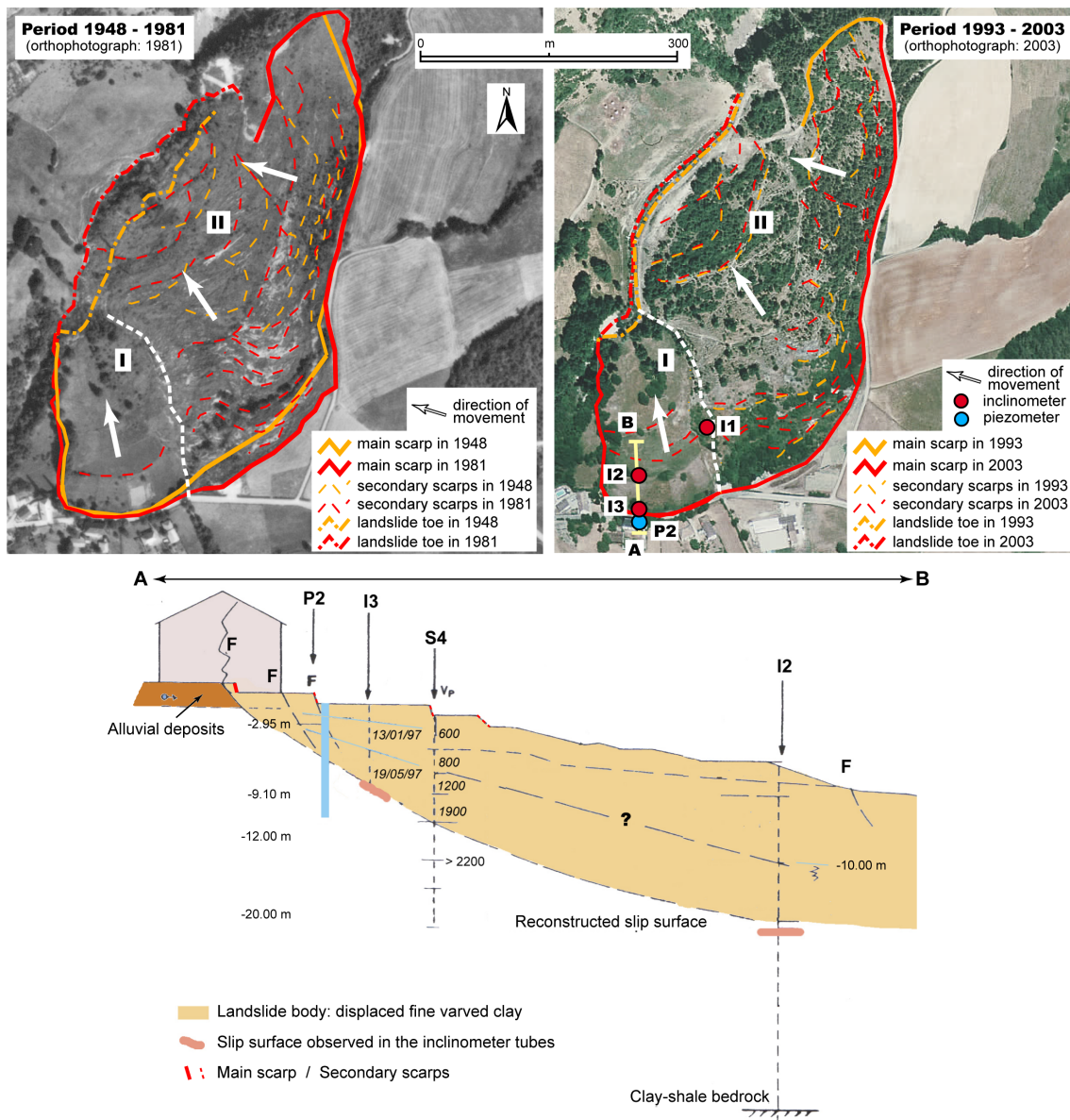


**Fig. 2.** Time evolution of the Monestier-du-Percy landslide reconstructed from aerial photographs, and cross section of the upper part of the landslide with the position of the reconstructed slip surface. The slip surface in the lower part is flat with a slope angle of about 13°. S4 is a seismic sounding, and the velocity profile of the P-waves are indicated for each layers. The position of the groundwater level observed at two dates in 1997 in P2 is also indicated.

- the South Western part (I in Fig. 2) is a landslide characterized by approximately 24 m of saturated clays and a slip surface located at –16 m below the main houses, and –9 m nearby the road. The groundwater levels can attain the topographic surface. This part of the slide affects three houses and the main road. In the 6-year period from 2000 to 2006, an average surface velocity of 5–20 mm yr<sup>-1</sup> is observed in this part of the landslide.
- the North-Eastern part (II in Fig. 2), of the landslide is moving faster, with an erosion of the main scarp of

10 m between 1978 and 1988. The bedrock is located at –40 m, and the slip surface at a depth of –20 to –25 m. This part of the landslide travelled a distance of more than 70 m in some points, and has displaced the position of the stream at the bottom of 30 m. In the 6-year period from 2000 to 2006, an average surface velocity of 30–60 mm yr<sup>-1</sup> is observed in this part of the landslide. Given the observed displacement rates, the landslide complex can be classified as very slow (Dikau et al., 1996).

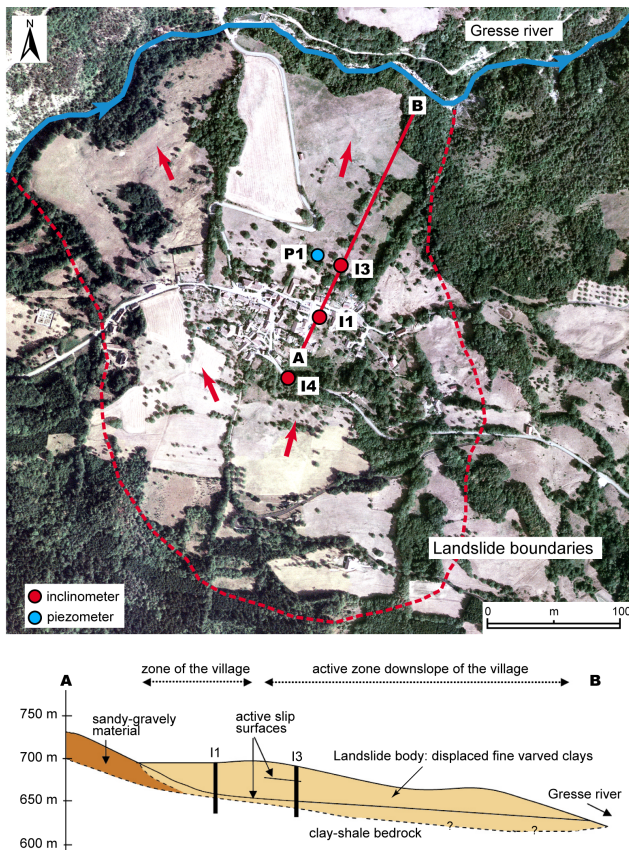


**Fig. 3.** Aerial photograph and supposed spatial limits of the Saint-Guillaume landslide in 2004, and schematic cross section through the village detailing the reconstructed slip surface and the position of inclinometers I3 and I4. The piezometer P1 is installed near inclinometer I3.

The measured displacement values in the field are consistent with the displacements calculated from the analysis of ortho-rectified aerial photographs for both parts of the landslide (I and II in Fig. 2) for two periods. In the South Western part of the landslide (I in Fig. 2), mean surface velocities of  $3\text{--}4\text{ mm yr}^{-1}$  are observed in the period 1948–1981, with a progression of the toe of 1 m, while mean surface velocities of  $50\text{ mm yr}^{-1}$  are observed in the period 1993–2003 with a displacement of the toe of 0.5 m. In the North Eastern part (II in Fig. 2), the landslide shows an attenuating trend in the displacement of the toe, of about 30 m (approximately  $1\text{ m yr}^{-1}$ ) in the period 1948–1981, and 3 m (approximately  $0.3\text{ m yr}^{-1}$ ) in the period 1993–2003.

Draining trenches and collectors have been installed in 1979 in order to drain the permeable alluvial deposits above the main scarp (Fig. 2) which are the main source of water for the landslide as direct rainfall amounts do not directly correlate to the groundwater levels. The water circulating in subsurface is also collected on the landslide with open gullies. A decrease in the velocity has been observed after the

main drainage works; however, the movements have not been stopped (Besson, 1996).

## 2.2 The Saint-Guillaume landslide

The Saint-Guillaume landslide is a slow ( $10\text{--}50\text{ mm yr}^{-1}$ ) translational landslide affecting the small village of Saint-Guillaume (Figs. 1c and 3). The geological basement is composed of Oxfordian clay-shale and marly limestone covered with 40 to 60 m of varved clays. The landslide has a length of 1.0–1.2 km, and a width of 0.5–0.8 km (Cravoissier, 2004). The main scarp in the upper part of the slope is not clearly visible but the hummocky topography and the development of fissures (along the road and in several buildings of the village) are indicators of the unstable terrain (Fig. 3).

The landslide is limited upslope (South) by a limestone cliff overhanging a scree hillslope (Fig. 3). Downslope (North), the landslide is limited by the Gresse river which incised a narrow channel in the varved clays. In the Eastern part, a geomorphological survey (geomorphological map, topographic control points) and a geotechnical investigation (three inclinometers and one piezometer) were carried out from the late 1990s (Guéguen et al., 2004). The results from the boreholes indicated the existence of an interface between the uppermost varved clays and the marly limestone bedrock at depths of 38.5 m, 62.0 m and 33.0 m for boreholes I1, I3 and I4, respectively (Fig. 3). The inclinometers detected slip surfaces inside the varved clays at 37.0 m, 34.5 m, and 14.0 m depth.

The monitoring system has been complemented since 2003 by a geophysical investigation (seismic noise measurements, seismic soundings, electrical resistivity tomography; Guéguen et al., 2004; Méric et al., 2007), yielding more spatially detailed information on the geometry and depth of the slip surface and the bedrock (Tatard, 2006). These results have suggested that the slip surfaces develop first at the clay/bedrock interface where the bedrock is close to the surface and then within the clay layer. This is confirmed by the inclinometer monitoring.

The landslide movement has been monitored since 1977 by 10 benchmarks in surface, and three inclinometers. Two active zones can be distinguished down slope of the village (Fig. 3); these two zones are limited by a positive undulation of the bedrock in the West-East direction in the central part of the landslide.

## 3 Description of the displacement models

Movement of a landslide is controlled by an excess of the driving forces over the Coulomb resisting forces which consist of the cohesion and friction of the material. It is common practice to subdivide the landslide body into slices and to calculate the forces for each slice  $i$  (Fig. 4). The difference between the driving force  $D_i$  and resisting force  $R_i$  (Fig. 4)

and the viscosity of the material determines the amount of displacement per time step for each slice  $i$ . Two model concepts have been selected to calculate the driving and resisting forces.

In the first concept, which is based on the Janbu equilibrium model (Janbu, 1954), the driving and resisting forces are calculated considering the weight  $W$  of the slice, the interlaminary forces acting on the sides of the slice, the normal force and mobilised shear resisting force acting respectively perpendicular and parallel to the slip surface (not depicted in Fig. 4). In a non-equilibrium situation, the driving force  $D_i$  is larger than the maximum resisting force  $R_i$ , which can be mobilized (Fig. 4). The safety factor  $F_i$  per slice, which expresses the degree of stability, is defined as the ratio between the maximum resting force  $R_i$  and driving factor  $D_i$ . Assuming a safety factor  $F_i$  per slice equals to the overall safety factor  $F$  for the whole landslide body, the following equilibrium equation was obtained by Janbu (1954) (Eqs. 1 and 2):

$$F = \frac{\sum R_i}{\sum D_i} = \frac{\sum [c' b_i + (W_i - u_i b_i) \tan \phi'] / n_{\alpha_i}}{\sum W_i \tan \alpha_i} \quad (1)$$

$$n_{\alpha_i} = \cos^2 \alpha_i \left( 1 + \tan \alpha_i \frac{\tan \phi'}{F_i} \right) \quad (2)$$

where for each slice  $i$ ,  $b_i$  is the width of the slice,  $W_i$  is the weight of the slice, and  $\alpha_i$  is the angle of the slip surface (Fig. 4);  $c'$  and  $\phi'$  are respectively the cohesion and angle of internal friction of the material. In the Janbu equation (Eq. 1), the effect of pore water pressure ( $u_i$ ) is included, and it decreases the resistance  $R_i$ .

The safety factor  $F$  on both sides of the equation has to be equalized by iteration, and  $R_i$  and  $D_i$  are calculated for each slice  $i$ . Then, the excess shear stress is calculated for slice  $i$  using Eq. (3):

$$(\tau - \tau_0)_i = \left( \frac{D_i - R_i}{l_i} \right) \quad (3)$$

where  $l_i$  is the length of the slip surface of slice  $i$  (Fig. 4). The excess shear stress for each point  $k$  along the vertical profile  $(\tau - \tau_0)_{i,k}$  within slice  $i$  can be calculated by assuming a linear relationship between the excess shear stress and height above the slip surface.

To model the displacements at specific points along the vertical  $z$ -profile (Fig. 4), the Coulomb viscous flow criterion is used. The incremental increase in velocity  $\Delta v_{i,k}$  for slice  $i$  at point  $k$  along the vertical profile  $z$  over an incremental height  $\Delta h$  is given by Eq. (4):

$$\Delta v_{i,k} = \frac{1}{\eta} (\tau - \tau_0)_{i,k} \Delta h \quad (4)$$

where  $\eta$  is the dynamic viscosity of the clays and  $(\tau - \tau_0)_{i,k}$  is the excess shear stress over the yield strength  $\tau_0$  at a certain point  $z_k$  along the vertical profile  $z$  within slice  $i$ . A

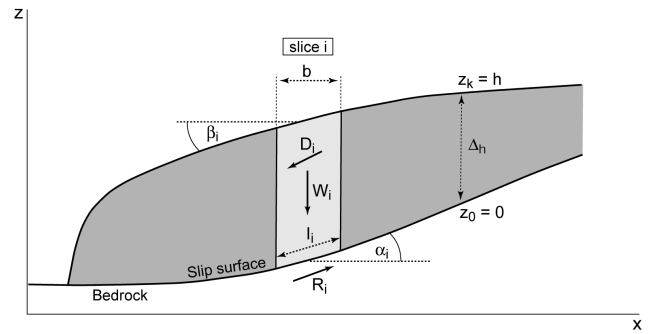


**Fig. 4.** Schematic scheme of a slice within a landslide showing the main forces and the symbols used in the two displacement models.

vertical velocity profile for each slice  $i$  can be calculated by integrating Eq. (4) over the depth  $z$ :

$$v_{i,k+1} = v_{i,k} + \Delta v_{i,k} \quad (5)$$

In the second model, the landslide is also subdivided in a number of slices (Fig. 4). In this case the forces are not solved on the basis of static conditions but by considering dynamic conditions of a moving landslide body. In this model concept, an internal pressure term  $P_i$  is formulated explicitly as part of the driving force  $D_i$  (Eq. 6) (Hung, 1995). The driving and resisting forces (Eqs. 6 to 9) are defined as follow:

$$D_i = G_i + P_i \quad (6)$$

$$G_i = W_i \sin \alpha_i \quad (7)$$

$$P_i = \kappa W_i \sin \alpha_i \tan \beta_i \quad (8)$$

$$R_i = c' l_i + (W_i \cos \alpha_i - u_i l_i) \tan \phi' \quad (9)$$

where  $D_i$  is the driving force and is the sum of the tangential component of the weight of the slice  $G_i$  and the tangential internal pressure component  $P_i$ . The internal pressure component  $P_i$  is a function of the lateral earth pressure coefficient  $\kappa$  (-) which is kept constant and the angle  $\beta_i$  of the topographical surface.

For each slice  $i$  the excess shear force is then given by Eq. (10):

$$(\tau - \tau_0)_i = \frac{D_i + P_i - R_i}{l_i} \quad (10)$$

The velocity in depth is then calculated according to Eqs. (4 and 5).

The main advantage of this model is that the three forces can be determined per slice without knowledge of the overall stability of the landslide. It means that there is no need to know the overall geometry of the landslide as is the case of the first model concept based on the Janbu equation. Only the geometry of the slice under consideration (Eqs. 7 to 9) has to be known.

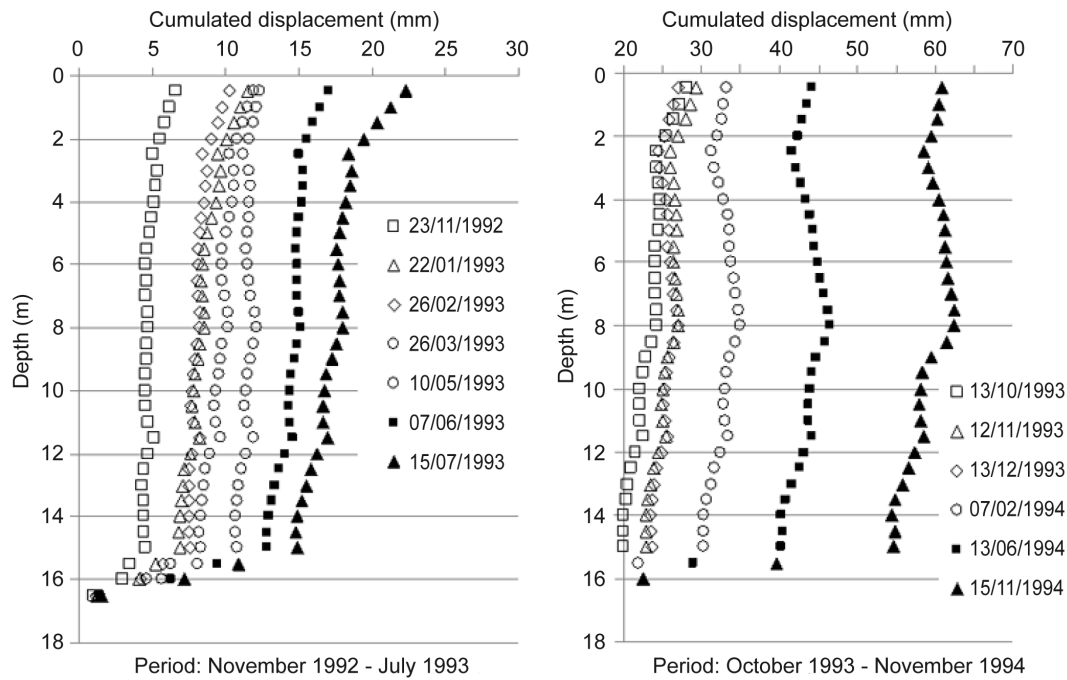


Fig. 5. Displacement profiles measured in inclinometer  $I_2$  at the Monestier-du-Percy landslide for the period 1992–1994.

## 4 Application of the displacement models

### 4.1 Analysis of the observed displacements along a vertical profile

Figure 5 shows the displacement profiles of inclinometer  $I_2$  at the Monestier-du-Percy landslide in the period 23 November 1992–15 November 1994, and Fig. 6 shows the displacement profiles of inclinometer  $I_2$  at the Saint-Guillaume landslide for two periods (21 February 1997–18 June 1998, and 16 October 2001–3 August 2005, respectively). The period between two measurements ranges between about 1 to 2 months in the first stage of the measuring campaign. When sufficient information on the rate of displacement was obtained, the period between two measurements was extended to 3 to 6 months (Figs. 5 and 6).

At the Monestier-du-Percy landslide, the maximum deformation near inclinometer  $I_2$  was found at a depth of around 15.5 m (Figs. 2 and 5). The total displacement over 3 years of measurements (not shown in Fig. 5) was about 88 mm which yields an average of about  $30 \text{ mm yr}^{-1}$ . The displacement profile over 2 years (Fig. 5) shows a deformation zone of less than 1 m thick with a more or less rigid plug with no internal shear deformation on top. The thickness of the deformation zone can be less than 1 m, but due to stiffness of the flexible tube, thinner shear layers cannot be detected. Thin shear layers develop where there are only narrow zones with excess shear stress (e.g.  $\tau - \tau_0 > 0$ ) or where the material has a pure plastic character without a viscous component (Carson, 1971). In the varved clays, more flow-like inclinometer pro-

files including thicker viscous deformation zones were detected as well for example on a landslide near La Mure (van Asch and van Genuchten, 1990) indicating a viscous component. These thicker deformation zones can develop with higher groundwater tables and/or steeper slopes. Figure 7 gives a theoretical example for the Monestier-du-Percy landslide. An increase of the groundwater level from  $-5.7 \text{ m}$  below the surface (which is a mean value measured in the field) to a hypothetical level of  $-3.5 \text{ m}$  below the surface will increase the thickness of the internal deformation zone. Figure 7 shows also the effect of an hypothetical slope angle ( $\alpha = 26^\circ$ ), on the increase in thickness of the deformation zone.

At the Saint-Guillaume landslide, the data from inclinometer  $I_3$  (Figs. 3 and 6) indicate the development of three deformation zones, at depths of  $-37 \text{ m}$ ,  $-33 \text{ m}$ , and  $-13 \text{ m}$ , respectively. The deformation zones are narrow bands of maximum 1 m, as for the Monestier-du-Percy landslide. The mean displacements at the surface were respectively 12 and  $8 \text{ mm yr}^{-1}$  for the two measuring periods (Fig. 6).

### 4.2 Hydrological observations

Only one groundwater observation per landslide is available, both in the upper part of the landslides (Figs. 2 and 3). Both instruments are standard open standpipes of 0.125 m in diameter. At the Monestier-du-Percy landslide, the piezometer was installed in a 10 m deep borehole with a filter between  $-5$  and  $-10 \text{ m}$  below the topographic surface, fully in the varved clays. At the Saint-Guillaume landslide, the

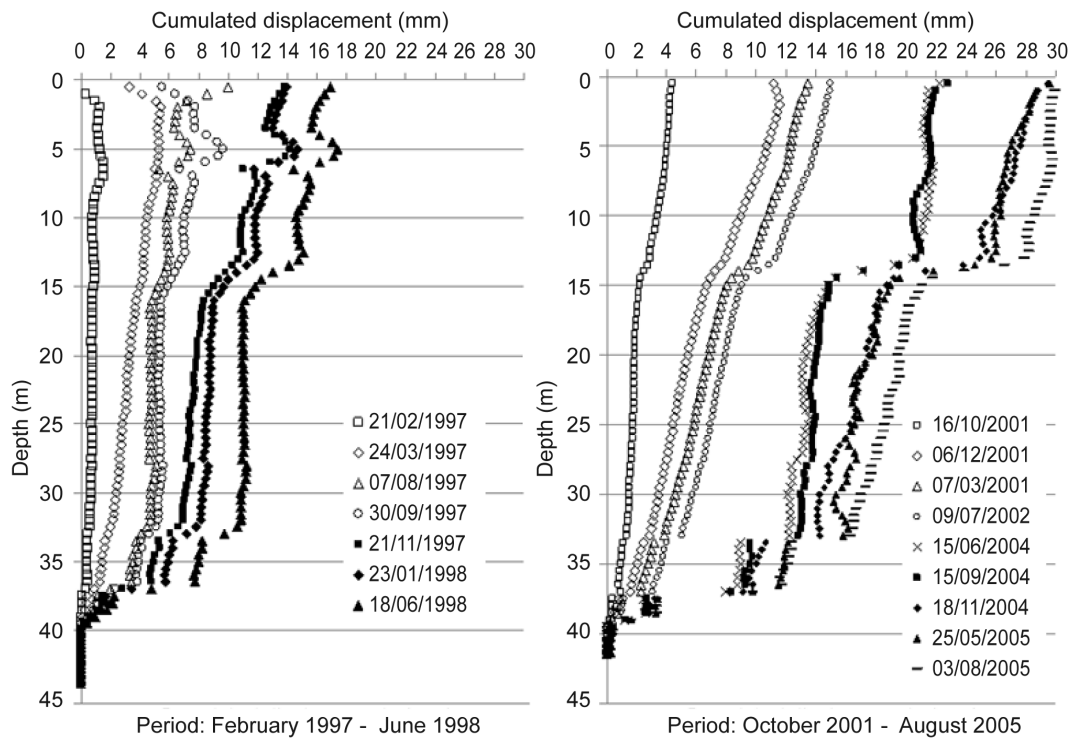


**Fig. 6.** Displacement profiles measured in inclinometer  $I_3$  at the Saint-Guillaume landslide for the period 1997–1998 and the period 2001–2005.

piezometer is located close to inclinometer  $I_3$  and has a 4 m filter between  $-5$  and  $-9$  m below the surface. Groundwater fluctuations are relatively small on both sites and range between 1 and 2 m.

The Monestier-du-Percy and Saint-Guillaume landslides show respectively groundwater levels (GWL) between  $-5$  and  $-6$  m below the surface, and between  $-4$  and  $-5$  m below the surface. The maximum groundwater levels are observed in April–May and November–December in both piezometers. As the varved clays have low saturated permeability values, it is important to estimate the hydrological lag time of the open standpipe piezometers before displacement and groundwater level can be related. Hvorslev (1951), Penman (1960), Dunnington (1988) and USACE (1995) proposed the use of a 90% recovery time of the open piezometers as a reasonable measure for the hydrostatic time lag, as 100% is infinite. The horizontal saturated permeability values for varved clays are estimated in the range of  $2.3$ – $4.6 \cdot 10^{-8} \text{ m s}^{-1}$  ( $2$ – $4 \text{ mm day}^{-1}$ ) (van Genuchten and van Asch, 1988; Vuillemet et al., 1994; van Asch et al., 1996). This gives a hydrostatic time lag ( $t_{90}$ ) for the two piezometers of 1 to 7 days. This relatively fast response is mainly due to the 4–5 m long filter lengths which are (almost) totally submerged in the groundwater system.

The fluctuation of the groundwater level in the varved clays may be regulated by a double hydrological reservoir system as was suggested by van Asch et al. (1996). The first

reservoir is a permeable alluvial/colluvial or morainic layer, of shallow thickness (1–3 m), which covers on most slopes the varved clays. The second reservoir is constituted by the fissure system in the varved clays which received the water from the first reservoir. The storage in the second reservoir of the fissure system determines the amount of horizontal water exchange between the fissures and the silt laminae of the varved clays (Nieuwenhuis, 1991; van Asch et al., 1996).

Figure 7 shows the fluctuation of the groundwater levels (measured per day) and the measured mean velocities for different periods between January 1993 and July 1995, obtained from displacement measurements with inclinometer  $I_2$  at the Monestier-du-Percy landslide. This figure shows a poor correlation between the two time series. There is no indication that velocity increases with rising groundwater levels. The same applies to the Saint-Guillaume landslide. The absence of correlation could have been influenced by the distance between the piezometers and inclinometers. However, precipitation is the main hydrological driver and is distributed equally over the landslide area. Further, there is no indication that the hydrological systems in varved clays have a groundwater wave passing through the landslide, resulting in time lags between observed groundwater dynamics and landslide activity.

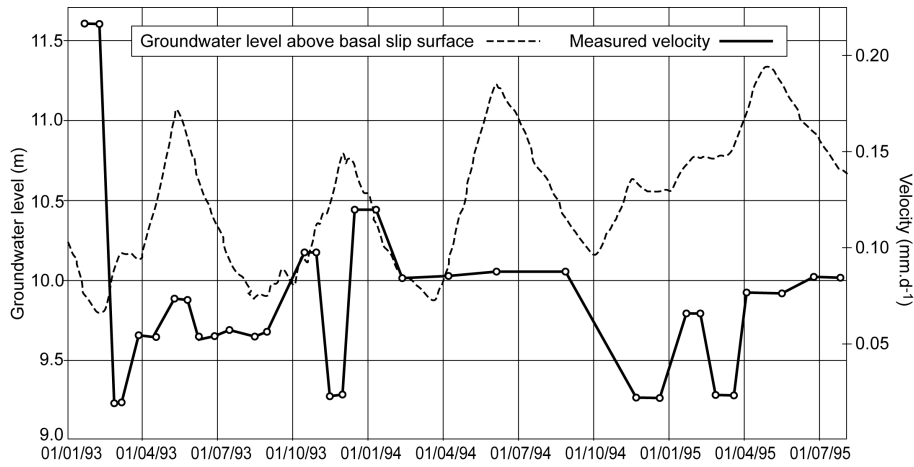


**Fig. 7.** Observed changes of the groundwater level (daily measurements) and mean measured velocities for different periods between January 1993 and July 1995 for the Monestier-du-Percy landslide.

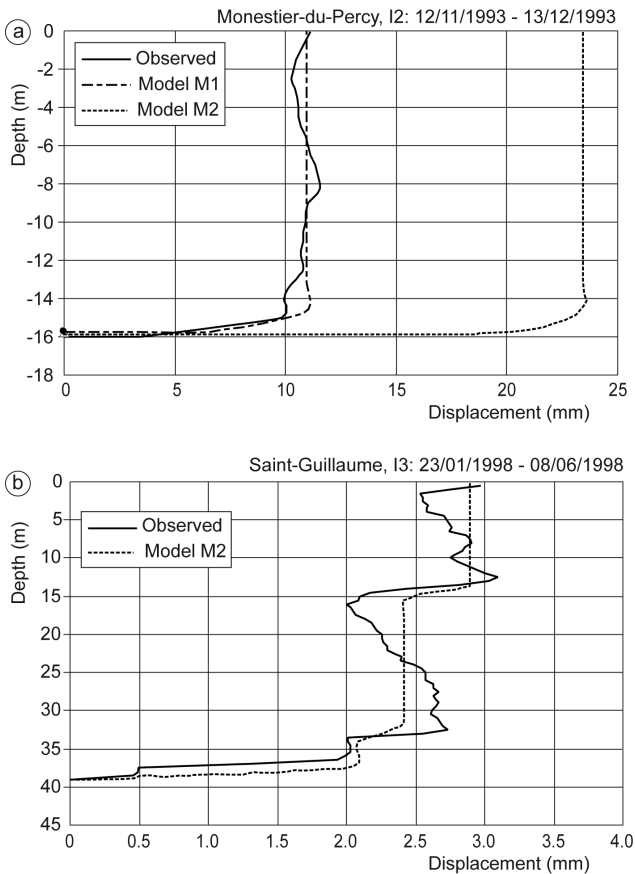


**Fig. 8.** Observed and simulated displacement profiles (a) for the Monestier-du-Percy landslide at inclinometer  $I_2$ , and (b) for the Saint-Guillaume landslide at inclinometer  $I_3$ .

### 4.3 Displacement modelling

The observed displacement profiles (Figs. 5 and 6) were used to calibrate the two models by using the friction angle of the varved clays as the calibration parameter. Giraud et al. (1991) presented cohesion values obtained from direct shear tests performed parallel to the laminae of the varved clays with peak values between 1 and 5 kPa and residual values of about 0 kPa. Therefore, the cohesion was assumed to be 0 in our modelling exercises. The viscosity (van Asch and van Genuchten, 1990; Giraud et al., 1991) is assumed to be constant for the measured period. For each measuring period, the mean groundwater level was calculated as input for the models. Figure 8a shows an example of a calibration result for the period 12 November 1993–13 December 1993 for the Monestier-du-Percy landslide with model M1 (Janbu). The calibrated friction value was  $\phi=21.2^\circ$  ( $c=0$  kPa,  $\eta=2.5 \times 10^8$  kPa s). Figure 9a indicates also the displacement profile calculated with the model M2 (equation of motion) using the same parametric values, which simulates a twofold higher displacement than model M1. A calibration with model M2 on the measured profile of Fig. 9a gives a friction value of  $\phi=21.4^\circ$ . Both models simulate a thin deformation zone with a large rigid plug on top, as was detected by the inclinometers.

Figure 8b describes an example of a calibration at the Saint-Guillaume landslide for the period 23 January 1998–8 June 1998. Calibration was performed with model M2. In order to simulate different slip surfaces, a variation of the friction angle and viscosity with depth was assumed. Calibration was performed from the bottom upwards. At each depth where a deformation zone was detected, a different friction angle was selected to fit the model with the observed displacements. Table 1 gives a summary of the calibrated parameters with depth. For the upper zone (between 0 and

**Table 1.** Calibrated parameters for the Saint-Guillaume landslide modelling exercise.

Depth (below surface, m)	$\phi$ ( $^{\circ}$ )	$\eta$ (kPa s)
0.0→−13.6	17.5	$6.0 \times 10^8$
13.6→−32.2	20.8	$2.5 \times 10^8$
32.2→−39.0	21.2	$2.5 \times 10^8$

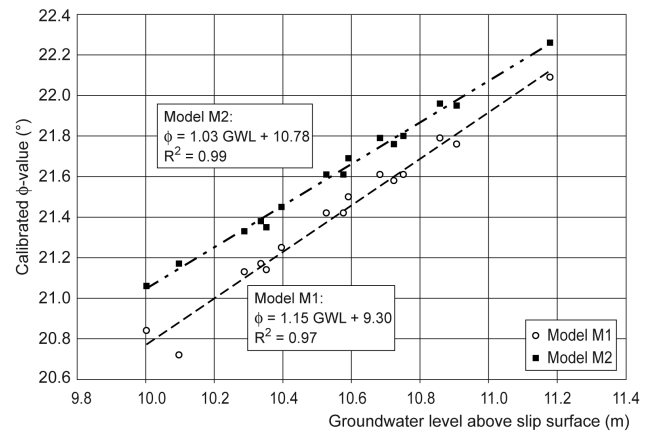
−13.6 m), it was necessary to calibrate the dynamic viscosity to a lower value than the one obtained from the literature.

The calibration with the  $\phi$  parameter did not give more or less constant values for both landslides: the  $\phi$ -values varied between 20.8 $^{\circ}$  and 22.3 $^{\circ}$  for the Monestier-du-Percy landslide and between 20.8 $^{\circ}$  and 21.2 $^{\circ}$  for the Saint-Guillaume landslide. These values are back calculated from several landslides with slip surfaces deeper than 15 m. Giraud et al. (1991) reported for samples taken at shallower depths (4 to 10 m) at three location in the Trièves area peak friction values ranging between 20 $^{\circ}$  and 21 $^{\circ}$  and residual values ranging between 18 $^{\circ}$  and 19 $^{\circ}$ . These measured residual values matches closely the back-calculated values for the Saint-Guillaume landslide for the depth until 13.6 m (Table 1), and the back-calculated values (friction angle between 17 $^{\circ}$ –19 $^{\circ}$ ) of the La Mure landslide with a slip surface at a shallow depth (4.5 m; van Genuchten and van Asch, 1988).

We may expect that a large part of the slip surfaces of the Monestier-du-Percy and Saint-Guillaume landslides are nearly parallel to the lamination of the clays, and that due to the movement the friction angles are in a residual state. In Fig. 9, the calibrated  $\phi$ -values are plotted against the mean groundwater level above the slip surface for different measuring periods at the Monestier-du-Percy landslide. A positive correlation is observed between the calibrated  $\phi$ -values and the pore water pressures. The same trend is observed at the Saint-Guillaume landslide. At higher pore water pressures, displacements appear to be regulated by the development of additional strength, which can be quantified as an apparent friction angle ( $\phi'$ ) that increases due to the generation of negative excess pore water pressures  $r_u$ :

$$\tan \phi' = (1 - r_u) \tan \phi_0 \quad (11)$$

The lowest friction angle was thus selected as the offset value  $\phi_0$  (Fig. 9), while the other calibrated  $\phi$ -values were considered as apparent friction angles ( $\phi'$ ). Based on these values, the excess pore water pressure coefficient  $r_u$  (kPa) can be calculated with Eq. (11). Excess negative pore water pressure varied between −1.0 and −24.3 kPa, depending on the groundwater level.

**Fig. 9.** Calibrated  $\phi$ -values ( $^{\circ}$ ) plotted against the mean groundwater level above the slip surface for different measuring periods at the Monestier-du-Percy landslide.

## 5 Discussion and conclusion

The Monestier-du-Percy and Saint-Guillaume landslides are typical examples of slow-moving and deep-seated landslides developed in varved clays. The deformation pattern showed a curved slip surface near the main scarp which transforms down slope in a straight plane with low slope angles. These landslides move over long time periods with varying (also zero) velocity. Over longer periods, a temporally attenuating trend in the amount of displacement seems to be observed at least for some parts of the Monestier-du-Percy landslide (Sect. 2.1). The overall decrease in velocity may be caused by an increase of the overall safety factor (Eq. 1) controlled by a loss of mass in the upper part of the landslide. This has an impact on the mean displacement rate over time.

The velocity profiles in both landslides show a relatively thin deformation zone of maximum 1 m in thickness. The two considered displacement models are able to simulate a relative thin viscous deformation zone with excess shear stress. On top of this thin deformation zone, a rigid plug with negative excess shear stress is observed and simulated. Thicker deformation zones, with an excess in shear stress over shear strength, can develop when the pore water pressure and/or the slope gradient increase (Fig. 10).

The increase in calibrated strength of the material with increasing pore water pressures was not expected. On the contrary, at lower pore water pressure values, the movement may stop and the consolidation of the material may lead to an increase in strength (Nieuwenhuis, 1991). The displacement velocity seems controlled by the intrinsic Coulomb-viscous resistance of the material and by the generation of excess (negative) pore water pressure during movement. Negative excess pore water pressure can be generated in extension zones of the landslide (Picarelli et al., 1995) where the material has the tendency to increase in volume (positive strain)

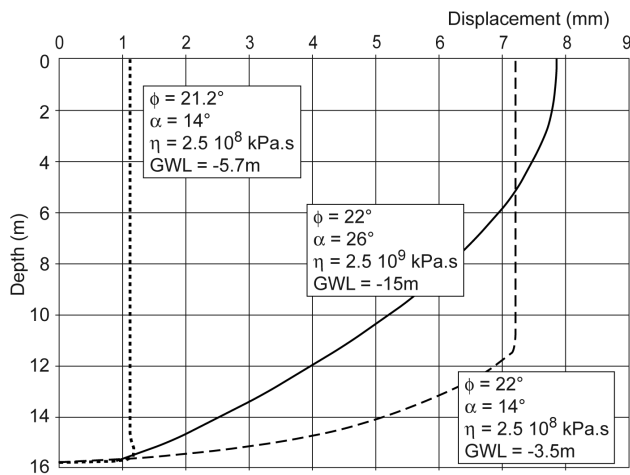


**Fig. 10.** Theoretical examples of modelled inclinometer profiles for different material strengths, groundwater levels (GWL), and slope conditions.

behind the distal sides of bumps in the slip plane (Keefer and Johnson, 1983) or due to dilation in the deformation zone (Iverson, 2005). Extension and compression zones were observed in slow-moving landslides in varved clays, e.g. by van Genuchten (1989) and Nieuwenhuis (1991).

It seems peculiar that both landslides show a positive correlation between a pore water pressure rise and an apparent strength regain by the generation of excess negative pore water pressure. On both sites, the inclinometers and piezometers were probably placed in a zone of extension. But the question arises whether these extension zones have such a lasting character as is the case of the Monestier-du Percy landslide.

This apparent feed-back mechanism of negative pore water pressure generation may (partly) be the result of time lag of the open standpipes to the groundwater fluctuation within the landslide. In case the piezometric groundwater level is higher than the soil pore water pressure, one measures a displacement velocity in relation with a groundwater level in the piezometer, which is in fact too high in relation to the observed velocity. This gives a quasi-apparent strength to the landslide mass at higher pore water pressure values, which are not yet in equilibrium with the pore water pressure in the landslide mass. At the opposite, the same is valid when measuring too low pore water pressures with open standpipes piezometers. Indeed, a relatively fast hydrological response of the piezometers of less than one week was calculated. Assuming, however, a tenfold lower lateral hydraulic conductivity, the 90% responses of the open standpipe piezometers are in the order of fifteen days but which could increase to one or two months in case of unfavourable, deviant effective filter geometry. This is valid with the assumption of an instantaneous pressure difference between the soil water pressure and the piezometer pressure. However, the period of

rising or falling limb of the groundwater level has a duration of 2 to 4 months over an height amplitude of 1 to 2 m. Therefore, it seems likely that the water level in the standpipe piezometers is more or less in equilibrium with the level in the landslide most of the time. More information is needed to analyse the hydrological mechanisms of water flows and generation of excess pore water pressures in the varved clays.

The feedback mechanisms may have been caused also by change in cohesion during movement. However the relative small fluctuation in groundwater level compared to the total depth let us assume that movement is more or less continuous throughout the year. This means that the cohesion remains nearly zero. Moreover, a slight increase of cohesion, due to an eventually short period of rest, has little impact on the total excess shear stress and hence the displacement rate, considering the large depth of the shear zone.

A change in the pressure term during movement may also cause this feedback effect in velocity (Eq. 8). It means that during a rise of groundwater level, the topographical slope (Eq. 8) has to decrease to give the counter effect. Despite the fact that we would expect rather an increase in the angle of friction, this geometrical change is so small over the fluctuation period that it has no influence on the displacement rate.

*Acknowledgements.* The authors thank D. Jongmans (LGIT, Grenoble) for delivering the inclinometer and piezometer data for both landslides, and the Pole Grenoblois des Risques Naturels for the implementation of the Trièves geotechnical database in 2006. They are also grateful to L. P. H. van Beek for his valuable suggestions in analyzing the data, and to F. Lindenmaier, two anonymous reviewers and the journal editor for their constructive comments of the manuscript.

Edited by: F. Guzzetti

Reviewed by: F. Lindenmaier and two other anonymous referees

## References

- Antoine, P., Giraud, A., and Monjuvent, G.: Les argiles litées du Trièves; conditions de glissement et exemples de propriétés géotechniques, *Bulletin Société Géologique de France*, 23(2), 117–127, 1981 (in French).
- Azimi, C., Biarez, J., Desvarreux, P., Giuliani, Y., and Ricard, C.: Mécanisme des glissements de terrains argileux – Bilan de surveillance sur plusieurs années, Internal Report, ADRGT, Grenoble, 1994.
- Besson, L.: Les risques naturels en montagne: traitement – prévention – surveillance. Editions Artès – Publialp, Grenoble, 1996 (in French).
- Carson, M. A.: The mechanics of erosion, London, Pion, 1971.
- Cravoisier, S.: Étude géophysique multi-méthodes d'un glissement de terrain en déformation lente: exemple des argiles de Saint Guillaume, Isère), MsC Thesis, Université Louis Pasteur, Strasbourg, 2004 (in French).
- Dikau, R., Brunnsden, D., Schrott, L., and Ibsen, M.-L.: Landslide recognition. Identification, movement and causes, John Wiley, Chichester, 1996.

- Giraud, A., Antoine, P., van Asch, Th. W. J., and Nieuwenhuis, J. D.: Geotechnical problems caused by glacio-lacustrine clays in the French Alps, *Eng. Geol.*, 31, 185–195, 1991.
- Dunnicliff, J.: Geotechnical instrumentation for monitoring field performance, John Wiley and Sons, Inc., New-York, 1988.
- Giraud, A., Gourc, J.-P., Besson, L., and Fabre, D.: Approche pluridisciplinaire des problèmes posés par un glissement de terrain sur faible pente, *Revue Française de Géotechnique*, 14, 11–15, 1980 (in French).
- Guéguen, P., Garambois, S., Cravoisier, S., and Jongmans, D.: Geotechnical, geophysical and seismological methods for surface sedimentary layers analysis, *Proceedings 3<sup>th</sup> World Conference of Earthquake Engineering*, Vancouver, Canada, 2004.
- Hvorslev, M. J.: Time lag and soil permeability in groundwater observations, *Bulletin No. 36*, US Army Engineer Waterways Experiment Station, Vicksburg, MS, 1951.
- Hungr, O.: A model for the runout analysis of rapid flow slides, debris flows and avalanches, *Canadian Geotechnical Journal*, 32, 610–623, 1995.
- Iverson, R. M.: Regulation of landslide motion by dilatancy and pore pressure feedback, *J. Geophys. Res.*, 110, F02015, doi:10.1029/2004JF000268, 2005.
- Janbu, N.: Application of composite slip surface for stability analysis, *Proceedings of the European Conference on the Stability of Earth Slopes*, 3, 43–49, 1954.
- Lorier, L. and Desvarreux, P.: Glissement de Monsetier-du-Percy – Serre-des-Bayles, *Proceedings of the workshop Ryskhydrogeo, Program Interreg III Alcotra, La Mure, France*, 2004 (in French).
- Keefer, D. K. and Johnson, A. M.: Earth flows-Morphology, mobilisation and movement, *US Geol. Surv. Prof. Pap.*, 1264, 1983.
- Méric, O., Garambois, S., Malet, J.-P., Cadet, H., Guéguen, P., and Jongmans, D.: Seismic noise based methods for soft rock landslide characterization, *Bulletin de la Société Géologique de France*, 178(2), 137–148, 2007.
- Nieuwenhuis, J. D.: Variations in stability and displacements of a shallow seasonal landslide in varved clays PhD Thesis, Utrecht University, Balkema, Rotterdam, 1991.
- Penman, A. D. M.: A study of the response time of various types of piezometers, *Proceedings of the Conference on Pore Pressures and Suction in Soils*, Butterworth, London, 1960.
- Picarelli, L., Russo, C., and Urcioli, G.: Modelling earthflow movement based on experiences. 11th European Conference on Soil Mechanics and Foundation Engineering, Copenhagen, 6, 157–162, 1995.
- Tatard, L.: Caractérisation et suivi du glissement de terrain de Saint Guillaume (Isère) par méthodes géophysiques, *MsC Thesis, University Joseph Fourier, Grenoble*, 2006 (in French).
- USACE: Engineering and Design: instrumentation of embankment dams and levee, *Engineering Manual, EM 1110-2-1908*, 1995.
- van Asch, Th. W. J. and van Genuchten, P. M. B.: A comparison between theoretical and measured creep profiles of landslides, *Geomorphology*, 3, 45–55, 1990.
- van Asch, Th. W. J., Hendriks, M. R., Hessel, R., and Rappange, F. E.: Hydrological triggering conditions of a landslide in varved clays in the French Alps, *Engineering Geology*, 42, 239–252, 1996.
- van Genuchten, P. M. B. and van Asch, Th. W. J.: Factors controlling the movement of a landslide in varved clays near La Mure (French Alps), *Bulletin de la Société Géologique de France*, 8(4), 461–469, 1988.
- van Genuchten, P. M. B.: On the temporal and spatial variance in displacement velocity of a slide in varved clays in the French Alps, *Earth Surf. Processes Landforms*, 14, 565–576, 1989.
- Vuillermet, E., Cordary, D., and Giraud, A.: Hydraulic characteristics of laminated clays in Trièves, France, *B. Eng. Geol. Environ.*, 49(1), 85–90, 1994.
- Vuillermet, E.: Caractéristiques géotechniques des argiles glacio-lacustres du Trièves, *PhD Thesis, University Joseph Fourier, Grenoble*, 1992 (in French).